Proceeding Paper

Microwave-Assisted Green Synthesis of Binary/Ternary $Zn_xCo_{1-x}Fe_2O_4$ (*x* = 0, 0.5, 1) Nanoparticles

Sanaz Chamani [1,*] and Masoumeh Khatamian [2]

[1] Koç University Boron and Advanced Materials Applications and Research Center (KUBAM), Istanbul 34450, Turkey
[2] Inorganic Chemistry Department, Faculty of Chemistry, University of Tabriz, Tabriz, Turkey; mkhatamian@yahoo.com
[*] Correspondence: schamani@ku.edu.tr
[†] Presented at the 28th International Electronic Conference on Synthetic Organic Chemistry (ECSOC 2024), 15–30 November 2024; Available online: https://sciforum.net/event/ecsoc-28.

Abstract: In this study, magnetic binary/ternary $Zn_xCo_{1-x}Fe_2O_4$ (*x* = 0, 0.5, 1) nanoparticles were synthesized using a straightforward one-step microwave technique. To produce the $Zn_xCo_{1-x}Fe_2O_4$ nanoparticles, Iron (III) nitrate nonahydrate, Zinc nitrate hexahydrate, and Cobalt nitrate hexahydrate were used as metal sources, with urea as the fuel and ammonium nitrate as the oxidizer. These materials were combined in an alumina crucible covered by a CuO jacket to absorb microwave energy and facilitate calcination. The thermal treatment involved placing the alumina crucible in a domestic microwave oven at 450 W for 30 min. The key strength of this experimental strategy includes its simplicity, cost-effectiveness, and rapidity, aligning with green chemistry principles. The synthesized nanoparticles were characterized using X-ray Diffraction (XRD), Fourier Transform Infrared spectroscopy (FT-IR), Vibrating Sample Magnetometer (VSM), and Brunauer-Emmett-Teller (BET) analysis. XRD analysis confirmed the presence of pure ferrite nanocrystalline phase. Scanning Electron Microscopy (SEM) equipped with Energy Dispersive X-ray Spectroscopy (EDS) was explored to study the surface morphology and analyze the elemental composition. The SEM analysis revealed that the synthesized magnetic nanoparticles have particle sizes ranging from 30 to 50 nm. Furthermore, the potential of these magnetic nanoparticles as photocatalysts for degrading organic pollutants such as methylene blue, in aqueous solutions was explored.

Keywords: microwave synthesis; magnetic nanoparticles; photocatalyst; organic pollutants

1. Introduction

Industrialization generates substantial toxic pollutants, including both organic and inorganic materials, particularly from the textiles, printing, and painting industries. Textiles release large amounts of azo dyes, which are vibrant, soluble, and stable. Given their toxicity and associated health risks, effectively removing these dyes from wastewater is essential [1–3]. Methods such as adsorption and photocatalysis have been used for dye removal from wastewater. Photocatalysts are increasingly favored due to their versatility, ease of use, and ability to operate under mild conditions. However, a key challenge with this method is the difficulty of separating the photocatalyst from the solution after dye degradation [2]. Magnetic metal ferrites have gained significant attention in recent years due to their catalytic, magnetic, and electromagnetic properties [4]. Several chemical techniques are available for synthesizing magnetic ferrite nanoparticles, including the sol-gel method [5], sol-gel auto-combustion method, hydrothermal method [6,7], microwave method [8,9], and co-precipitation method [10]. Among these methods, the microwave method has attracted significant interest due to its advantages, including feasibility, low cost, environmental friendliness, and short reaction time. In this work, we synthesized

magnetic binary/ternary $Zn_xCo_{1-x}Fe_2O_4$ (x = 0, 0.5, 1) nanoparticles using the microwave method. We investigated the efficacy of these nanoparticles as photocatalysts for the degradation of methylene blue in aqueous solutions.

2. Experimental Section

All chemicals, obtained from Merck Co., were utilized directly without further purification.

Synthesis of binary/ternary $Zn_xCo_{1-x}Fe_2O_4$ (x = 0, 0.5, 1) nanoparticles:

We employed a one-step microwave technique to synthesize binary/ternary $Zn_xCo_{1-x}Fe_2O_4$ (shown in Figure 1). $Fe(NO_3)_3 \cdot 9H_2O$, $Co(NO_3)_2 \cdot 6H_2O$, and $Zn(NO_3)_2 \cdot 6H_2O$ served as the metal sources, with NH_2CH_2COOH as the fuel and NH_4NO_3 as the oxidizer. For the preparation of $Zn_{0.5}Co_{0.5}Fe_2O_4$ nanoparticles, a mixture containing $Fe(NO_3)_3 \cdot 9H_2O$ (2 mmol), $Co(NO_3)_2 \cdot 6H_2O$ (0.5 mmol), $Zn(NO_3)_2 \cdot 6H_2O$ (0.5 mmol), NH_2CH_2COOH (3 mmol), and NH_4NO_3 (6 mmol) was first prepared. The mixture was then transferred to an alumina crucible surrounded by a CuO jacket to absorb microwave energy and provide calcination heat. Thermal treatment was carried out in a domestic microwave oven operating at 450 W for 30 min. The resulting powder was collected, washed several times with distilled water and ethanol to remove residual materials, and dried at 80 °C for 24 h. A similar procedure was followed for the synthesis of $ZnFe_2O_4$ and $CoFe_2O_4$.
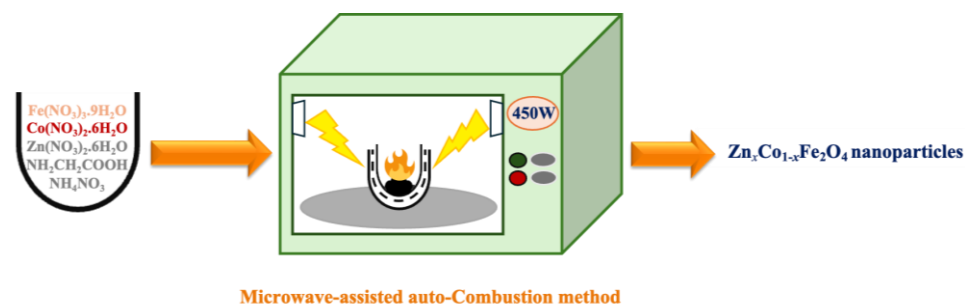
Figure 1. Schematic representation of the synthesis method.

3. Result and Discussion

Figure 2a illustrates the reflected characteristic peaks of the $Zn_xCo_{1-x}Fe_2O_4$ nanoparticles. The peaks at 2θ values approximately 18.41°, 30.29°, 35.68°, 37.33°, 43.37°, 53.82°, 57.37°, 62.7°, and 74.57° correspond to the (111), (220), (311), (222), (400), (422), (511), (440), and (533) planes, respectively. These findings confirm the presence of a single-phase cubic spinel structure without any secondary phases, in good agreement with JCPDS card no. 77-0426 for $CoFe_2O_4$. It should be noted that the dashed line around 2θ of 62.7 shows a peak shift to smaller 2θ values as the Zn content increases. This shift indicates Zn substitution in the $CoFe_2O_4$ structure, resulting in larger lattice parameters (see Figure 2b).

The creation of $Zn_xCo_{1-x}Fe_2O_4$ nanoparticles was confirmed using Fourier transform infrared (FT-IR) analysis. Figure 3a shows two metal–oxygen (M–O) absorption bands in the 400–600 cm^{-1} range: bands from 500–600 cm^{-1} indicate metal stretching at tetrahedral sites, and bands below 450 cm^{-1} correspond to metal stretching at octahedral sites. No additional absorption bands from organic groups were observed. The magnetic properties of $Zn_xCo_{1-x}Fe_2O_4$ nanoparticles were measured using a vibrating sample magnetometer (VSM) at room temperature as shown in Figure 3b. Various magnetic characteristics, such as saturation magnetization (Ms), coercivity (Hc), and remanence magnetization (Mr), were determined from the hysteresis loops. The obtained values are detailed in Table 1. Based on the results, $ZnFe_2O_4$ and $Zn_{0.5}Co_{0.5}Fe_2O_4$ exhibit low coercivity (Hc) and narrow hysteresis loops, indicating that these materials are soft magnetic materials. In contrast,

$CoFe_2O_4$ displays a wide hysteresis loop, signifying that it is a hard magnetic material. It was also observed that $CoFe_2O_4$ has the highest saturation magnetization (Ms) value of 66.4 emu/g and the highest coercivity (Hc) of 1174.5 Oe.
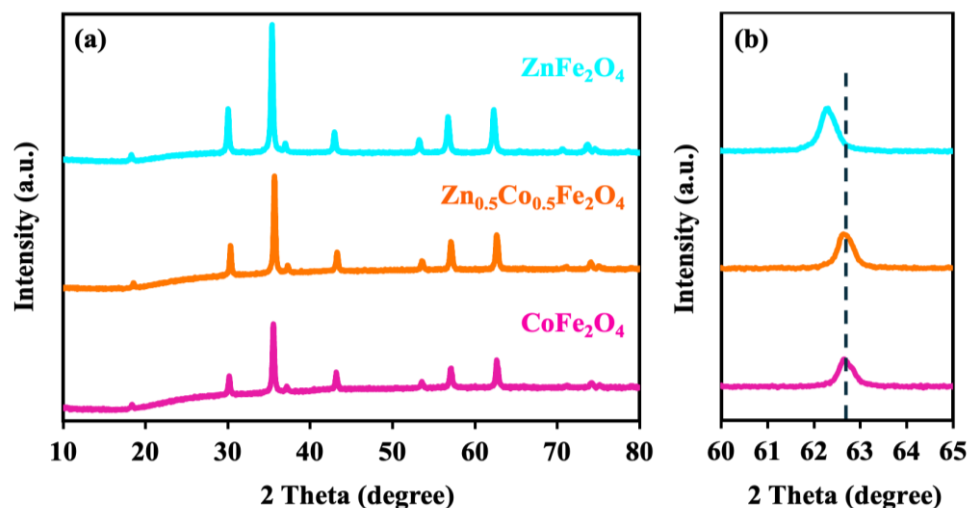

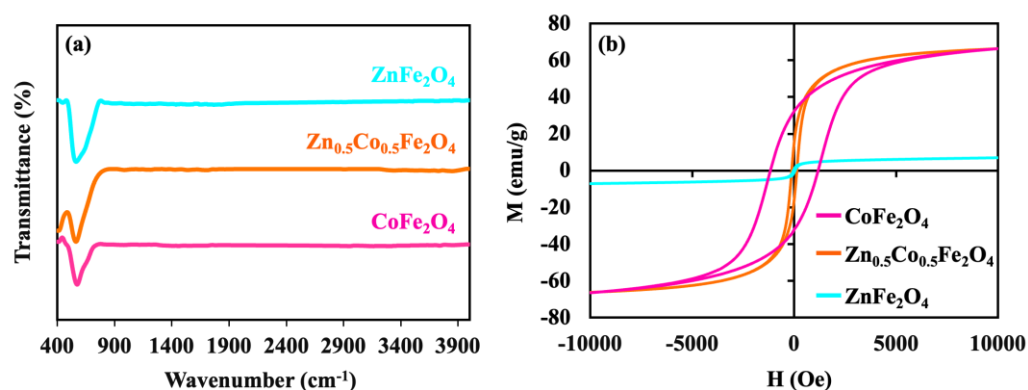**Figure 2.** (**a**,**b**) XRD patterns of as-prepared magnetic nanoparticles.

Figure 3. (**a**) FT-IR spectra and (**b**) Magnetization curve of as-prepared magnetic nanoparticles.

Table 1. Variation of Ms, Hc, and Mr of Spinel $Zn_xCo_{1-x}Fe_2O_4$ (*x* = 0, 0.5, 1) nanoparticles.

Sample	Ms	Hc	Mr
$CoFe_2O_4$	66.4	−1174.5	32.5
$Zn_{0.5}Co_{0.5}Fe_2O_4$	66.3	−128.4	16
$ZnFe_2O_4$	7	47.5	1.2

Surface morphology and elemental composition were investigated using SEM equipped with EDS. The SEM images in Figure 4 reveal that the synthesized magnetic nanoparticles have sizes ranging from 30 to 50 nm. The observed agglomeration of particles is likely due to the magnetic properties inherent in the prepared ferrite nanoparticles. The surface area of the magnetic nanoparticles was measured using multi-point Brunauer–Emmett–Teller (BET) analysis. The BET surface areas were found to be 11.35 m^2/g for $CoFe_2O_4$, 8.3 m^2/g for $Zn_{0.5}Co_{0.5}Fe_2O_4$, and 8.5 m^2/g for $ZnFe_2O_4$, respectively.
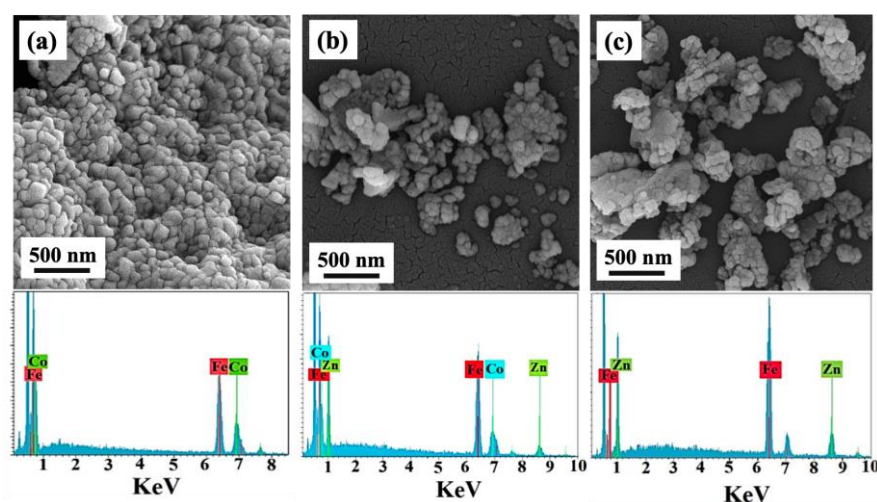
Figure 4. SEM/EDS images of (**a**) $CoFe_2O_4$, (**b**) $Zn_{0.5}Co_{0.5}Fe_2O_4$, and (**c**) $ZnFe_2O_4$.

4. Photocatalytic Activity

The photocatalytic properties of magnetic binary/ternary $Zn_xCo_{1-x}Fe_2O_4$ nanoparticles in the degradation of methylene blue were investigated at room temperature. In a typical procedure, 50 mL of 20 ppm methylene blue solution were combined with 50 mg of the catalyst and stirred magnetically both before and during illumination. The suspension was agitated in the dark for 30 min to maximize dye adsorption onto the catalyst surface. After that, the mixture was exposed to UV light for three hours. Samples of methylene blue solution were taken after 30min, 60min, 120 min, 180 min and 240 min respectively and the absorbance of methylene blue after each time interval was tested using a UV-Vis spectrophotometer at 650 nm. The degradation efficiency was calculated using the following equation:

$$\text{Degradation efficiency \%} = (C_0 - C_t)/C_0$$

where C_0 represents the initial concentration of methylene blue (mg/L), and C_t is the methylene blue concentration (mg/L) at various irradiation times t. The degradation of efficiency depends on the ability of absorption, the generation of electron-hole pairs and the ability of diffusion and separation of electron hole pairs [1].

Figure 5 illustrates the time-dependent extent of methylene blue degradation, revealing an enhancement in dye degradation at various time intervals for all prepared $Zn_xCo_{1-x}Fe_2O_4$ nanoparticles. The removal efficiencies for methylene blue were 48%, 51%, and 33% for zinc ion concentrations of $x = 0$, 0.5, and 1, respectively. Figure 5 shows that degradation efficiency increases over time, with $Zn_{0.5}Co_{0.5}Fe_2O_4$ achieving the highest degradation among all samples. This improvement can be attributed to the doping of Zn into the $CoFe_2O_4$ structure, which creates more surface oxygen vacancies and defects, thereby enhancing the photocatalytic degradation process.
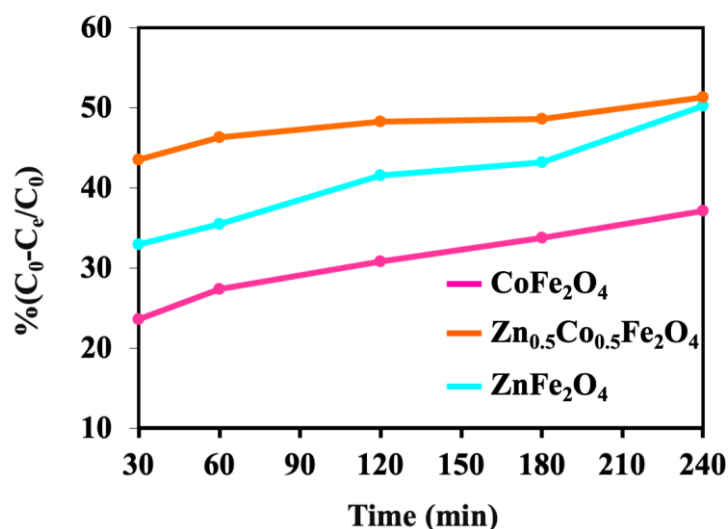
Figure 5. Degradation efficiency of methylene blue dye in the Presence of magnetic nanoparticles.

5. Conclusions

In summary, magnetic binary/ternary $Zn_xCo_{1-x}Fe_2O_4$ (x = 0, 0.5, and 1) nanoparticles were successfully synthesized using a one-step microwave auto-combustion method. The XRD patterns confirm that all the as-prepared magnetic nanoparticles exhibit a single-phase cubic spinel structure. The SEM analysis revealed that the synthesized magnetic nanoparticles have particle sizes ranging from 30 to 50 nm and showed agglomeration at the nanoscale due to their magnetic properties. The potential of these magnetic nanoparticles as photocatalysts for degrading methylene blue in aqueous solutions was investigated. The removal efficiencies for methylene blue dye were observed to be 48%, 51%, and 33% for zinc ion concentrations of x = 0, 0.5, and 1, respectively. The photocatalytic study indicated that among the prepared photocatalysts, $Zn_{0.5}Co_{0.5}Fe_2O_4$ exhibited the highest degradation efficiency. These findings demonstrate that cobalt zinc ferrite can serve as an effective photocatalyst for methylene blue degradation, without posing any hazardous effects on the environment.

References

1. Chahar, D.; Taneja, S.; Bisht, S.; Kesarwani, S.; Thakur, P.; Thakur, A.; Sharma, P.B. Photocatalytic activity of cobalt substituted zinc ferrite for the degradation of methylene blue dye under visible light irradiation. *J. Alloys Compd.* **2021**, *851*, 156878.
2. Kamel Attar Kar, M.; Fazaeli, R.; Manteghi, F.; Ghahari, M. Structural, Optical, and Isothermic Studies of $CuFe_2O_4$ and Zn-Doped $CuFe_2O_4$ Nanoferrite as a Magnetic Catalyst for Photocatalytic Degradation of Direct Red 264 Under Visible Light Irradiation. *Environ. Prog. Sustain. Energy* **2019**, *38*, 13109.
3. Swathi, S.; Yuvakkumar, R.; Kumar, P.S.; Ravi, G.; Velauthapillai, D. Annealing temperature effect on cobalt ferrite nanoparticles for photocatalytic degradation. *Chemosphere* **2021**, *281*, 130903.
4. Magdalane, C.M.; Priyadharsini, G.M.A.; Kaviyarasu, K.; Jothi, A.I.; Simiyon, G.G. Synthesis and characterization of TiO_2 doped cobalt ferrite nanoparticles via microwave method: Investigation of photocatalytic performance of congo red degradation dye. *Surf. Interfaces* **2021**, *25*, 101296.

5. Alshammari, A.H.; Alshammari, K.; Alhassan, S.; Alshammari, M.; Alotaibi, T.; Alanzy, A.O.; Taha, T.A.M. Low temperature sol-gel synthesis of copper zinc ferrite for hydrogen catalytic hydrolysis of sodium borohydride. *Mater. Chem. Phys.* **2023**, *308*, 128287.

6. Bashar, A.; Molla, T.H.; Chandra, D.; Malitha, D.; Islam, S.; Rahman, S.; Ahsan, S. Hydrothermal synthesis of cobalt substitute zinc-ferrite ($Co_{1-x}Zn_xFe_2O_4$) nanodot, functionalised by polyaniline with enhanced photocatalytic activity under visible light irradiation. *Heliyon* **2023**, *9*, 1538.

7. Kaur, N.; Katoch, A.; Singh, S.; Kaur, R. Properties of zirconium ferrite nanoparticles prepared by hydrothermal process. *Mater. Lett.* **2023**, *330*, 133236.

8. Chamani, S.; Khatamian, M.; Peighambardoust, N.S.; Aydemir, U. Microwave-Assisted Auto-Combustion Synthesis of Binary/Ternary $Co_x Ni_{1-x}$ Ferrite for Electrochemical Hydrogen and Oxygen Evolution. *ACS Omega* **2021**, *6*, 33024–33032.

9. Chamani, S.; Sadeghi, E.; Peighambardoust, N.S.; Doganay, F.; Yanalak, G.; Eroglu, Z.; Aslan, E.; Asghari, E.; Metin, O.; Patir, I.H.; et al. Photocatalytic hydrogen evolution performance of metal ferrites/polypyrrole nanocomposites. *Int. J. Hydrogen Energy* **2022**, *47*, 32940–32954.

10. Charles Prabakar, A.; Sathyaseelan, B.; Killivalavan, G.; Iruson, B.; Senthilnathan, K.; Manikandan, E.; Sivakumar, D. Photocatalytic dye degradation properties of zinc copper ferrites nanoparticles. *J. Nanostruct.* **2019**, *9*, 694–701.